

ARTICLE

Supporting Information

Unravelling the charge state of gold on partially reduced ceria thin films

Luchao Huang,^a Qian Xu,^{*a} Erbao Cao,^a Jun Hu,^a and Junfa Zhu^{*a, b}

a. National Synchrotron Radiation Laboratory, University of Science and Technology of China, Hefei 230029, P. R. China

b. Department of Chemical Physics, Key Laboratory of Surface and Interface Chemistry and Energy Catalysis of Anhui Higher Education Institutes, and Key Laboratory of Precision and Intelligent Chemistry, University of Science and Technology of China, Hefei 230026, P. R. China.

*Corresponding Author, Email: qianxu@ustc.edu.cn; jfzhu@ustc.edu.cn

The amount of deposited gold was calculated using the following method:

Just as described in the experimental section, all the experiments were conducted in two separate ultra-high vacuum (UHV) systems. Both experimental beamlines are equipped with XPS, SRPES, and LEED, allowing us to perform XPS measurements to determine the amount of gold deposited, thereby ensuring consistent gold coverage across experiments conducted on different setups.

In this work, the Au coverage on CeO_x(111) was determined by quantifying the amount of deposited Au. The Au deposition rate was monitored by quartz crystal microbalance (QCM) and then calibrated by the attenuation of Ru 3d XPS signal after depositing Au directly onto the Ru(0001) surface at low coverage. The reason we chose the Ru(0001) substrate is that Au grows in a layer-by-layer fashion at least for the first two layers on Ru(0001) single crystal^{1, 2}. The calculated deposition rate of Au is 0.12 Å/min.

The exact amount of Au deposited onto CeO_x(111) is calculated by multiplying the deposition rate by the evaporation time assuming unit sticking probability of Au on CeO_x(111). Because Au grows as 3D nanoparticles on CeO_x(111) at room temperature, we thus adopt the very common monolayer definition of metal nanoparticles on oxide surfaces^{3, 4}. One monolayer (ML) of Au is defined as 1.39×10^{15} atoms/cm², which is the number of Au atoms per area in a close-packed (111) layer of bulk Au crystal. In this work, the amount of Au deposited is manifested by monolayers. The monolayer thickness is calculated by the number of Au atoms per area divided by the number of Au atoms per volume (5.90×10^{22} atoms/cm³) in bulk Au, which is 2.35 Å.

Since we know the deposition rate and can control the Au deposition time, the exact deposited Au amount can be obtained and converted to monolayers. For example, to prepare a 0.50 ML Au/CeO_x(111) sample, with a deposition rate of 0.12 Å/min, the required deposition time was 9.83 minutes. Therefore, the amount of Au is 0.12 Å/min \times 9.83 minutes = 1.18 Å. As 1 ML thickness is 2.35 Å, thus, the coverage is calculated to be 1.18/2.35 = 0.5 ML.

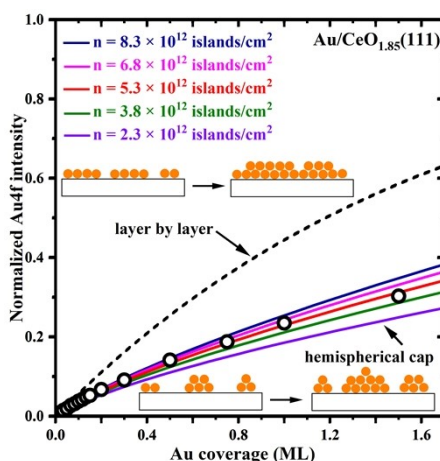


Figure S1. Integrated Au 4f intensity normalized to that of bulk Au versus coverage for Au growth on a 2-4 nm thick $\text{CeO}_{1.85}(111)$ film grown on $\text{Cu}(111)$ at room temperature (open circles). The dashed black curve corresponds to what is expected if Au grows in a layer-by-layer growth mode, and the other curves represent a hemispherical cap model with a constant island density, n . The inelastic mean free path used for calculation is 0.4 nm for Au, obtained from Ref. 5.

According to the 3D particle (hemispherical cap) growth model^{6,7}, the intensity ratios are given as follows:

$$\frac{I_{\text{Au}}}{I_{\text{Au}}(\infty)} = nR^2\pi - 2\pi n\lambda_{\text{Au}}^2 \left[1 - \left(1 + \frac{R}{\lambda_{\text{Au}}} \right) e^{-\frac{R}{\lambda_{\text{Au}}}} \right] \quad (1)$$

where I_{Au} represents the Au 4f intensity and $I_{\text{Au}}(\infty)$ is the Au intensity from a thick bulklike Au layer on $\text{CeO}_{1.85}(111)$, d is the Au thickness, λ_{Au} is the mean free path of Au photoelectrons, R and n are the radius and the number density of the hemispherical Au particles, respectively.

We assume the gold grows on $\text{CeO}_{1.85}(111)$ in a 3D mode like hemispherical cap. Therefore, $d=2/3nR^3\pi$. The number of particle density n then becomes the only fitting parameter. It should be noted that in the hemispherical cap model, the number of particle density is assumed to be independent of coverage and treated as a constant for fitting. Therefore, the fitted curve is derived for a given n . Figure S1 presents fitting curves for different values of n , showing that deviation from the experimental data occurs if the particle density n increases above or decreases below 5.3×10^{12} islands/ cm^2 . Instead, the signal is in excellent agreement with the hemispherical cap model, assuming a constant particle density of 5.3×10^{12} islands/ cm^2 .

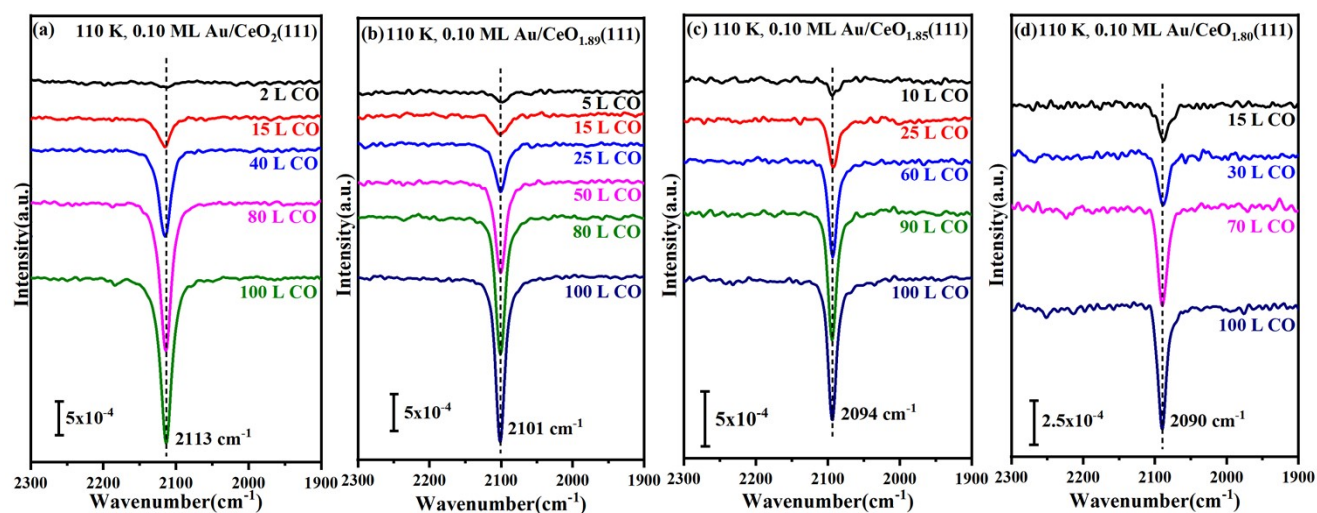


Figure S2. IRAS spectra obtained from the Au/CeO₂(111) (a), Au/CeO_{1.89}(111) (b), Au/CeO_{1.85}(111) (c), and Au/CeO_{1.80}(111) (d) surfaces with incremental doses of CO at 110 K.

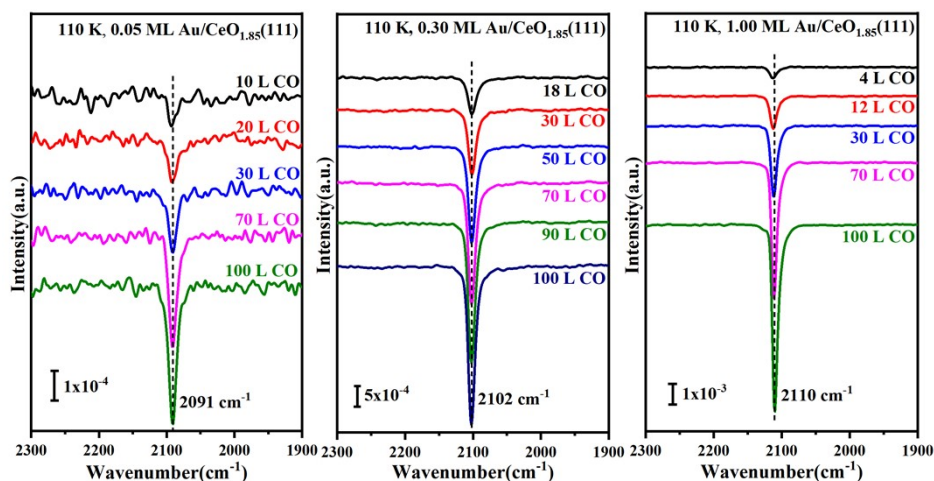


Figure S3. IRAS spectra obtained from the CeO_{1.85}(111) surface with different Au coverages with incremental doses of CO at 110 K.

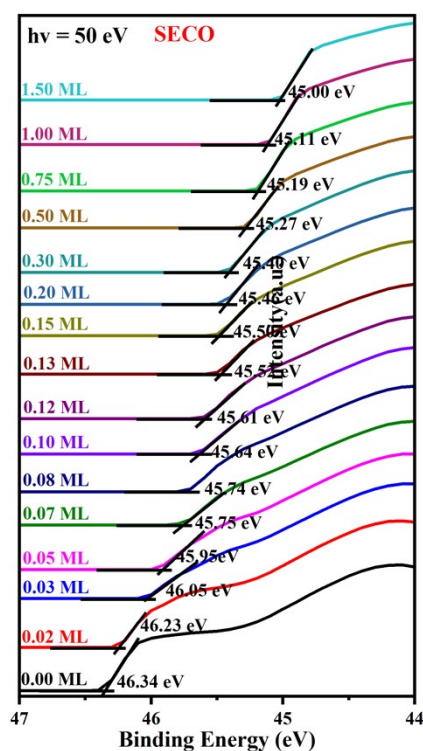


Figure S4. Secondary electron cutoff spectra at different Au coverages.

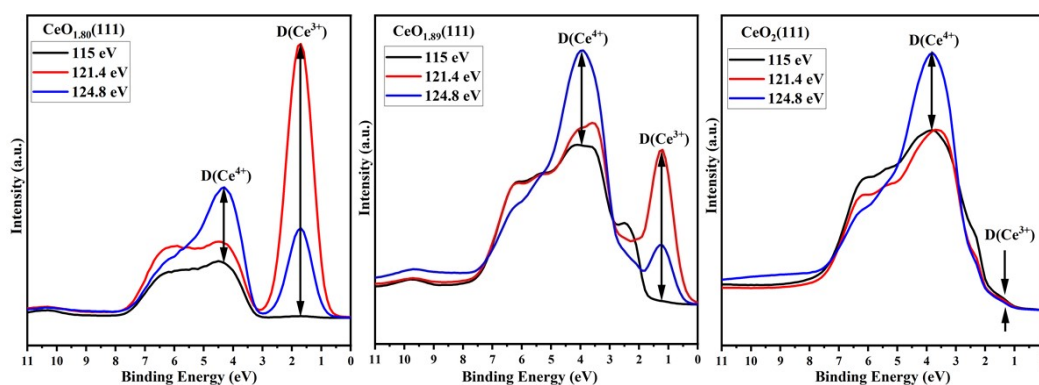


Figure S5. Resonant photoemission valence band spectra acquired on the $\text{CeO}_x(111)$ surface at different photon energies: 115 eV (off-resonance, black lines), 121.4 eV (Ce^{3+} resonance, red lines), and 124.8 eV (Ce^{4+} resonance, blue lines). The resonant enhancements for Ce^{3+} (denoted as $D(\text{Ce}^{3+})$) and for Ce^{4+} ($D(\text{Ce}^{4+})$) are quantified by calculating the intensity difference between the corresponding features on- and off-resonance as indicated by black arrows.

The resonant enhancement ratio (RER) is defined as $D(\text{Ce}^{3+})/D(\text{Ce}^{4+})$. The Ce^{3+} concentration can be calculated from RER via the formula: $n(\text{Ce}^{3+})/n(\text{Ce}^{4+}) = \text{RER}/y$, $y=5.5$.⁸ The stoichiometry of ceria was thus determined via the formula⁸:

$$x = 2 - \frac{1}{2} \frac{n(\text{Ce}^{3+})}{n(\text{Ce}^{3+}) + n(\text{Ce}^{4+})}$$

Reference:

- [1] G. Pötschke; J. Schröder; C. Günther; R. Q. Hwang; R. J. Behm, *Surf. Sci.* **1991**, 251-252, 592-596.
- [2] J. Schröder; C. Günther; R. Q. Hwang; R. J. Behm, *Ultramicroscopy* **1992**, 42-44, 475-482.
- [3] E. Wahlström; N. Lopez; R. Schaub; P. Thosttrup; A. Rønnau; C. Africh; E. Lægsgaard; J. K. Nørskov; F. Besenbacher, *Phys. Rev. Lett.* **2003**, 90, 026101
- [4] D. Matthey; J. G. Wang; S. Wendt; J. Matthiesen; R. Schaub; E. Lægsgaard; B. Hammer; F. Besenbacher, *Science* **2007**, 315, 1692-1696.
- [5] S. Tanuma; C. J. Powell; D. R. Penn, *Surf. Interface Anal.* **1988**, 11, 577-589.
- [6] U. Diebold; J. M. Pan; T. E. Madey, *Phys. Rev. B* **1993**, 47, 3868-3876.
- [7] J. Zhu; J. A. Farmer; N. Ruzycski; L. Xu; C. T. Campbell; G. Henkelman, *J. Am. Chem. Soc.* **2008**, 130, 2314-2322.
- [8] Y. Lykhach; S. M. Kozlov; T. Skála; A. Tovt; V. Stetsovych; N. Tsud; F. Dvořák; V. Johánek; A. Neitzel; J. Mysliveček; S. Fabris; V. Matolín; K. M. Neyman; J. Libuda, *Nat. Mater.* **2015**, 15, 284-288.